INFECTION AND IMMUNITY, Jan. 1995, p. 356–359 Vol. 63, No. 1
0019-9567/95/$04.00+0

Rapid Disruption of Epithelial Barrier Function by *Salmonella typhimurium* Is Associated with Structural Modification of Intercellular Junctions

MARK A. JEPSON,* CARLA B. COLLARES-BUZATO, M. ANN CLARK, BARRY H. HIRST, AND NICHOLAS L. SIMMONS

Department of Physiological Sciences, Medical School, University of Newcastle upon Tyne, Newcastle upon Tyne NE2 4HH, United Kingdom

Received 1 August 1994/Returned for modification 8 September 1994/Accepted 1 October 1994

Short-term infection of MDCK II monolayers with *Salmonella typhimurium* SL1344 caused a progressive decrease in transepithelial electrical resistance concomitant with decreased cation permselectivity and increased paracellular inulin flux. Cytochemical staining of F-actin, E-cadherin, and ZO-1 revealed the concentration of each junctional protein in invaded cells as a result of contraction at their apical poles and resultant distortion of adjacent uninvaded cells.

Invasion of cultured mammalian cells by *Salmonella typhimurium* involves a complex range of cytoskeletal and membrane alterations that make up a process termed membrane ruffling (7–11). This is believed to occur as a response to the triggering of signal transduction pathways (10, 11, 13, 15, 17), although the precise stimulus for these changes remains subject to debate and may differ in detail between cell lines (10). The majority of research in this field has involved the use of nonpolarized epithelioid cell lines such as HeLa and Henle-407, although the rapid induction by *S. typhimurium* of similar cytoskeletal alterations and membrane blebs in polarized epithelial cell lines such as MDCK and Caco-2 (9, 12) suggests that similar mechanisms are involved in the invasion of these cells.

Infection of polarized monolayers of epithelial cells (MDCK and Caco-2) with *Salmonella* species has also been shown to elicit a decrease in transepithelial electrical resistance (7, 8). The mechanisms underlying this phenomenon are unknown, although an increased paracellular permeability has been demonstrated in MDCK monolayers after prolonged (15-h) infection with *S. typhimurium* (2). Because prolonged time courses were used in these previous studies, the relationship between the observed increase in paracellular permeability and the more immediate cellular responses to *Salmonella* infection which lead to membrane ruffling (9, 12) remain unclear.

To elucidate the mechanisms underlying the effects of *Salmonella* species on epithelial barrier function, we have examined the consequence of short-term *S. typhimurium* infection of MDCK monolayers on the function and morphology of intercellular junctions.

S. typhimurium SL1344 (provided by C. L. Francis, Stanford University, Stanford, Calif.) was grown as previously described (4), reproducing conditions shown to enhance invasiveness (9), and diluted to 10^8/ml (3×10^7 to 6×10^7 CFU/ml) in modified Krebs buffer (137 mM NaCl, 5.4 mM KCl, 1 mM $MgSO_4$, 0.3 mM KH_2PO_4, 0.3 mM NaH_2PO_4, 2.4 mM $CaCl_2$, 10 mM glucose, and 10 mM Tris, adjusted to pH 7.4 at 37°C with HCl) supplemented with 10% (vol/vol) heat-inactivated fetal calf serum. Madin-Darby canine kidney (MDCK) strain II cells (passage 116 to 122) (1) cultured on permeable Anocell tissue culture inserts (effective growth area, 0.5 cm^2) as described previously (6) for 3 days were equilibrated in modified Krebs buffer (as above) for 30 to 60 min at 37°C in air and then exposed to the bacterial suspension (0.5 ml) at their apical surface. Infected monolayers were maintained for up to 60 min at 37°C in air, during which time the transepithelial electrical resistance was monitored as previously described (6). A progressive decrease in transepithelial electrical resistance (R_T) was evident as early as 15 min after the initiation of infection; by 60 min, infected monolayers displayed R_Ts of 40 to 70% that of control monolayers; e.g., in a representative experiment, the R_T of monolayers 60 min after *S. typhimurium* infection was 47.67 ± 5.11 Ω cm^2 (mean ± standard deviation, $n = 6$) compared with 85.25 ± 5.15 Ω cm^2 ($n = 6$) for control monolayers (significant difference by Student's t test, $P < 0.001$). No alteration in R_T occurred in monolayers incubated in medium containing an equivalent volume of filtered *S. typhimurium* culture broth. The drop in R_T induced by *S. typhimurium* was associated with a decrease in the cation permselectivity of the epithelial monolayers measured as a decrease in the sodium: choline bi-ionic potential difference (Table 1), which was evident within the first 15 min of infection and was more pronounced by 60 min. Direct evidence of increased paracellular permeability in *S. typhimurium*-infected MDCK monolayers was provided by an increased flux of the extracellular marker [^{14}C]inulin, measured as described previously (5). Increased inulin flux was already evident 30 min after initiation of infection (0.198% ± 0.040% of apically applied inulin appeared in basal medium, in contrast to 0.098% ± 0.006% for control monolayers) and was further enhanced by 60 min (0.446% ± 0.092% of inulin crossing infected monolayers, in contrast to 0.196% ± 0.012% for control monolayers). These results are mean ± standard deviation of six experiments, and the results for infected monolayers are significantly different from those for control ($P < 0.05$ by the Mann-Whitney U test).

To gain insight into the mechanisms underlying the *S. typhimurium*-induced increase in paracellular permeability, the architecture of intercellular junctions in *S. typhimurium*-infected MDCK strain II monolayers was examined by confocal laser scanning microscopy in conjunction with cytochemical techniques. Staining of *S. typhimurium*-infected monolayers with

* Corresponding author. Mailing address: Department of Physiological Sciences, Medical School, University of Newcastle upon Tyne, Newcastle upon Tyne NE2 4HH, United Kingdom. Phone: 091 222 7772. Fax: 091 222 6706.

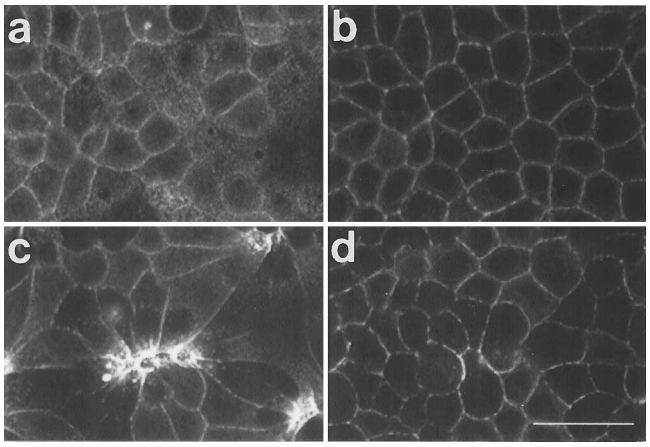

FIG. 1. Phalloidin staining of control (a and b) and *S. typhimurium* SL1344-infected (60 min) (c and d) MDCK monolayers. Images were obtained with a Bio-Rad MRC-600 confocal laser scanning microscope equipped with an argon laser and attached to a Nikon Optiphot microscope. Confocal optical sections at the level of apical surface and intercellular junctions (a and c) and 6 μm below this point (b and d) reveal regular brush border and circumferential distribution of F-actin in control monolayers (a and b) and the clear accumulation of perijunctional F-actin in discrete regions of the *S. typhimurium*-infected monolayer (c). Note the uneven cell shape, with elongated cells radiating in a stellate pattern around contracted cells displaying intense staining of perijunctional F-actin. Below the level of the intercellular junctions, a more normal cell morphology is observed in *S. typhimurium*-infected monolayers (d). Identical imaging parameters were used to allow comparison between control and *S. typhimurium*-infected monolayers. Bar, 25 μm.

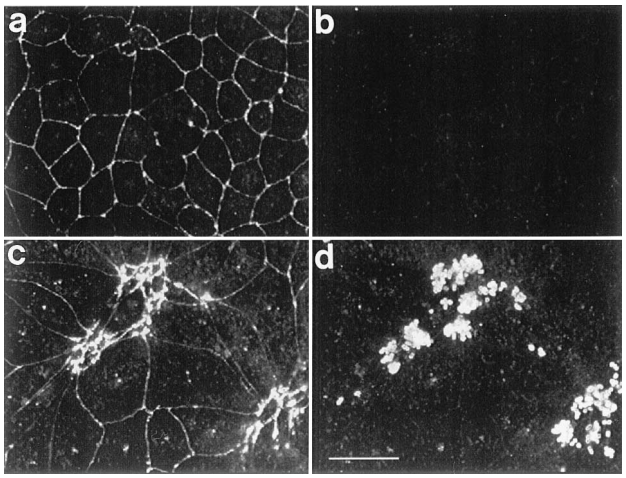

FIG. 2. Dual immunofluorescent staining of MDCK monolayers with antibodies against the tight-junction protein ZO-1 (a and c) and *Salmonella* species (b and d). Images were obtained with a Bio-Rad MRC-600 confocal laser scanning microscope equipped with a krypton/argon laser and attached to a Nikon Diaphot inverted microscope. Images are projections of confocal optical sections (to a 10-μm depth) collected with constant imaging parameters to enable direct comparison between control (a and b) and *S. typhimurium*-infected (c and d) monolayers. Control monolayers display an even distribution of ZO-1 around the circumference of MDCK cells (a) and absence of *Salmonella* cells (b). *S. typhimurium* infection (60 min) results in a distinct accumulation of ZO-1 (c) in regions of the monolayer associated with *Salmonella* cells (d). The projection of a series of optical sections allows simultaneous observation of surface-associated and invading *Salmonella* cells (d). Uninvaded MDCK cells surrounding the intensely stained regions are enlarged by the contraction of infected MDCK cells at their apical pole (c). Bar, 25 μm.

TRITC-phalloidin as described previously (6) revealed marked alterations of F-actin reorganization compared with control monolayers, which included the appearance of intracellular accumulations of F-actin corresponding to the presence of invading bacteria (data not shown). In addition, more-striking, intensely labeled accumulations of perijunctional F-actin were present throughout the monolayer (Fig. 1); they appeared as focal points from which elongated cells with an apparently normal complement of F-actin radiated in a stellate pattern (Fig. 1). Examination of confocal optical sections at and below the level of the junctional complex revealed this pattern of perijunctional F-actin staining to be due to constriction of the cells at their apical poles, which causes a gross distortion of the apical regions of neighboring uninvaded cells; optical sections beneath the level of the junctional complex revealed a more even cell morphology closely resembling that of control cell monolayers (Fig. 1).

Immunocytochemical staining of the adherens junction component E-cadherin and tight-junction component ZO-1 (as described previously [6]) revealed similar distributions, with each of these proteins being present at enhanced levels in regions of infected monolayers which, after dual staining with anti-*Salmonella* antibodies (CSA-1) and TRITC-labelled rabbit anti-goat immunoglobulin G (Sigma; 1:100) by a modification of a previously described technique (4), were invariably found to correspond to the positions of groups of invading bacteria (Fig. 2 and 3). As with phalloidin staining, these intensely labelled regions were surrounded by a radiating pattern of elongated cells. In monolayers immunostained to localize E-cadherin, which is expressed throughout the lateral membrane, *Salmonella* invasion was clearly associated with constriction of cells at their apical poles, a more regular cell morphology being apparent beneath the level of the junctional complex (Fig. 3 and 4).

The described alterations in the distribution of each of these key junctional components, F-actin, E-cadherin, and ZO-1, were already evident after 15 min of infection but were more pronounced by 60 min. The observed contraction of the apical circumferential junctional ring of *S. typhimurium*-infected cells and consequent distortion of the apical regions of adjacent cells were also apparent by scanning and transmission electron-microscopic examination of infected monolayers. These gross changes in cell morphology were closely associated with structural degeneration of the apical brush border and distortions of the apical membrane consistent with membrane ruffling as previously described for cultured epithelial monolayers (9, 12).

Our observations that short-term infection of strain II MDCK monolayers with *S. typhimurium* SL1344 induces a decrease in R_T concomitant with an increase in the transepithelial flux of inulin extend the results of a previous report

TABLE 1. Sodium:choline bi-ionic potential difference across *S. typhimurium*-infected and untreated MDCK monolayers[a]

Time (min) postinfection	Potential difference (mV)[b] for:	
	Control	*S. typhimurium* SL1344
0	38.87 ± 2.19 (3)	39.03 ± 0.82 (3)
15	33.07 ± 2.07 (3)	21.93 ± 1.20 (3)*
60	32.47 ± 1.41 (3)	14.90 ± 1.28 (3)*

[a] Cation permselectivity was measured as the potential difference across MDCK II monolayers exposed apically to standard Krebs buffer without fetal calf serum and basally to Krebs buffer in which NaCl was isoosmotically replaced by choline chloride.

[b] Results are expressed as mean ± standard error (n) bi-ionic potential difference (Na^+:choline) after subtraction of the basal potential difference (measured across monolayers with NaCl present in both bathing media). Asterisks denote a significant difference between control and *S. typhimurium*-infected monolayers by Student's unpaired t test ($P < 0.01$).

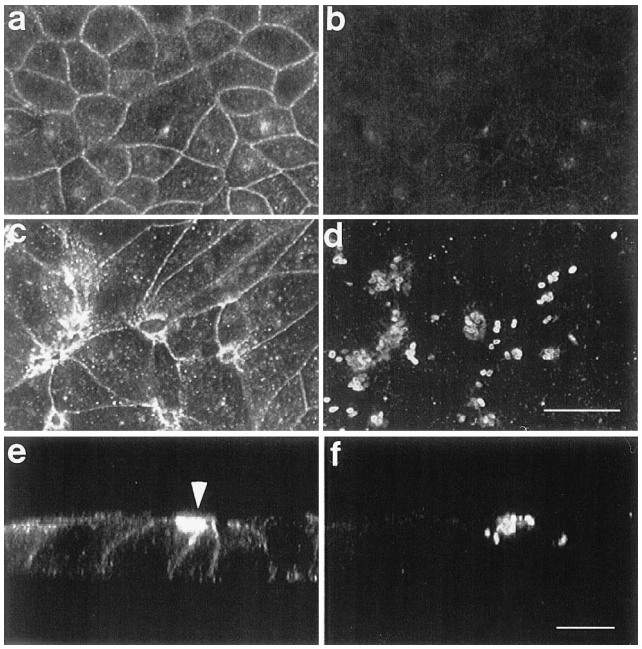

FIG. 3. Dual immunofluorescent staining of MDCK monolayers with antibodies against the adherens junction protein E-cadherin (a, c, and e) and *Salmonella* species (b, d, and f). Images were obtained with a Bio-Rad MRC-600 confocal laser scanning microscope equipped with a krypton/argon laser and attached to a Nikon Diaphot inverted microscope. Confocal optical section at the level of the apical surface of control monolayers (a and b) reveals regular distribution of E-cadherin in the lateral membrane (a) and the absence of *Salmonella* cells (b). Monolayers infected with *S. typhimurium* SL1344 for 60 min (c and d) display regions of intense E-cadherin staining (c) which are closely associated with invading *Salmonella* cells (d) and are surrounded by uninvaded MDCK cells with an elongated profile (c). Images were collected at equivalent sensitivities to enable direct comparison between control and *S. typhimurium*-infected monolayers. Confocal optical sections perpendicular to the plane of the monolayer (*X-Z* images [e and f]) show constriction of the apical portion of *S. typhimurium*-infected MDCK cells (arrowhead) leading to distortion of the apical region of neighboring (uninvaded) MDCK cells. Bars, 25 μm (a to d) and 10 μm (e and f).

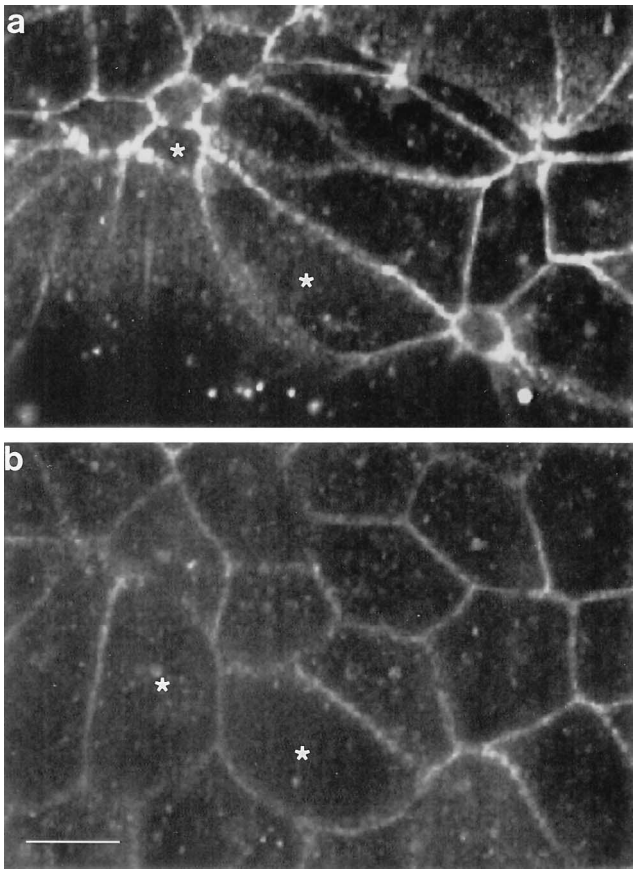

FIG. 4. Immunofluorescent E-cadherin staining of MDCK monolayers 60 min after infection with *S. typhimurium* SL1344. Images were obtained with a Bio-Rad MRC-600 confocal laser scanning microscope equipped with an argon laser and attached to a Nikon Optiphot microscope. An optical section at the apical pole (a) reveals intense labelling around the periphery of a subpopulation of cells and distortion (stretching) of neighboring cells. (b) An optical section 4 μm below that in panel (a) reveals regular cell morphology, demonstrating that distortions of cell shape are restricted to the apical pole. Asterisks indicate the presence of two cells in each optical section to aid interpretation. Scale bar, 25 μm.

documenting increased paracellular flux of inulin after a prolonged (15-h) infection of strain I MDCK monolayers with *S. typhimurium* SL1344 (2). Because the marker inulin provides a definition of the magnitude of the paracellular flux component, these data clearly demonstrate that a functional opening of the paracellular pathway is likely to be involved in the observed decrease in R_T induced by *S. typhimurium*. In addition, a decrease in the cation permselectivity of the epithelium is observed; the most likely explanation for this is disruption of the high-conductance paracellular route. Alternatively, the induction of a transepithelial secretory chloride conductance might contribute to this phenomenon. The possible involvement of a transcellular component in the decrease in cation permselectivity and/or transepithelial resistance that is coincident with the increase in paracellular inulin flux will have to be assessed in studies in which the relative ionic conductance of the apical (transcellular) route and the paracellular pathway are measured. However, it is clear that short-term infection with *S. typhimurium* produces a dynamic change in the functional properties of the epithelium.

Where is the exact location of the increased paracellular permeability observed in *S. typhimurium*-infected epithelial monolayers? Histochemical analysis failed to detect discontinuities in the distribution of the intercellular junction components F-actin, E-cadherin, and ZO-1 such as have been described after various treatments which enhance paracellular transport in MDCK monolayers such as calcium chelation and treatment with polycations (5, 6, 14). The present studies do, however, demonstrate gross morphological distortions in the region of intercellular junctions of infected MDCK cells. Additionally, the contraction of infected cells gives rise to gross torsional rearrangement of the apical portions of neighboring, uninvaded, cells. These two separate loci are both likely to contribute to the observed increase in the paracellular permeability of infected monolayers. This conclusion is supported by the fact that the incidence of these morphological alterations followed a similar time course to that of the observed increase in paracellular transport. It should be noted that the junctional effects of *S. typhimurium* infection are unlike those induced by inhibition of protein tyrosine phosphatases by treatment of MDCK monolayers with sodium vanadate and hydrogen peroxide, in which widespread loss of E-cadherin staining from intercellular junctions was apparent (5). This may argue against a simple relationship between the *S. typhimurium*-induced increase in paracellular transport and nonspecific tyrosine phosphorylation of junctional proteins, e.g., as a consequence of activation of the epidermal growth factor receptor

(10, 11, 15), but it cannot exclude an involvement of receptor activation and/or protein phosphorylation.

The rapid (15- to 60-min) time course of the *Salmonella*-induced modulation of paracellular transport reported here is consistent with its being associated with bacterial invasion and/or membrane ruffling, which have been shown to occur within minutes of infection in MDCK cells (9, 12; also see above). The described alterations in epithelial barrier function may result from the triggering of signal transduction pathways, e.g., growth factor activation, protein phosphorylation, phospholipase activation, and increased intracellular calcium and inositol phosphate fluxes, all of which have been described during invasion of other cell lines (e.g., HeLa and Henle-407) by *S. typhimurium* (10, 11, 15, 17). Indeed, some of these components of the signalling pathways previously demonstrated or inferred to be stimulated by *S. typhimurium* increase paracellular permeability in MDCK cells, e.g., activation of phospholipase C and protein kinase C (3, 18), increased intracellular calcium levels (16), and an increase in protein tyrosine phosphorylation (5). At present there is a paucity of information regarding the precise signalling events occurring in MDCK cells following *S. typhimurium* infection, while it is known that *Salmonella* species induce different signalling events in a variety of nonpolarized cell lines (10).

It is not yet known whether the above-described reorganization of intercellular junctions in MDCK monolayers has in vivo correlates. In murine intestinal loops, where *S. typhimurium* SL1344 preferentially invades M cells within the follicle-associated epithelium (4), extensive membrane ruffling was not apparently associated with contraction of *S. typhimurium*-associated M cells or distortion of neighboring enterocytes. It is now of interest to determine whether distortions in intercellular junctions occur after *S. typhimurium* invasion of absorptive enterocytes, which has also been shown to occur in vivo (19), and to assess the importance of these alterations in epithelial barrier function in intestinal invasion in vivo.

We are grateful to M. Geggie for assistance with cell culture.

M.A.J. was supported by Wellcome Trust Postdoctoral Fellowship 039684/Z/93/Z. C.B.C.-B. was supported by CAPES Fellowship 1887/91-1 (Brazil) and ORS Award 9129002 (United Kingdom). M.A.C. was supported under the LINK Programme in Selective Drug Delivery and Targeting funded by BBSRC/MRC/DTI and industry (SERC grant GR/F 09747). Additional support for equipment was provided by The Royal Society (grant 11761).

REFERENCES

1. **Barker, G., and N. L. Simmons.** 1981. Identification of two strains of cultured canine renal epithelial cells (MDCK cells) which display entirely different physiological properties. Q. J. Exp. Physiol. **66:**61–72.
2. **Canil, C., I. Rosenshine, S. Ruschkowski, M. S. Donnenberg, J. B. Kaper, and B. B. Finlay.** 1993. Enteropathogenic *Escherichia coli* decreases the transepithelial electrical resistance of polarized epithelial monolayers. Infect. Immun. **61:**2755–2762.
3. **Citi, S.** 1992. Protein kinase inhibitors prevent junction dissociation induced by low extracellular calcium in MDCK epithelial cells. J. Biol. Chem. **117:** 169–178.
4. **Clark, M. A., M. A. Jepson, N. L. Simmons, and B. H. Hirst.** 1994. Preferential interaction of *Salmonella typhimurium* with mouse Peyer's patch M cells. Res. Microbiol. **145:**543–552.
5. **Collares-Buzato, C. B., M. A. Jepson, G. T. A. McEwan, N. L. Simmons, and B. H. Hirst.** 1994. Junctional uvomorulin/E-cadherin and phosphotyrosine-modified protein content are correlated with paracellular permeability in Madin-Darby canine kidney (MDCK) epithelia. Histochemistry **101:**185–194.
6. **Collares-Buzato, C. B., G. T. A. McEwan, M. A. Jepson, N. L. Simmons, and B. H. Hirst.** 1994. Paracellular barrier and junctional protein distribution depend on basolateral Ca^{2+} in cultured epithelia. Biochim. Biophys. Acta **1222:**147–158.
7. **Finlay, B. B., and S. Falkow.** 1990. *Salmonella* interactions with polarized human intestinal Caco-2 epithelial cells. J. Infect. Dis. **162:**1096–1106.
8. **Finlay, B. B., B. Gumbiner, and S. Falkow.** 1988. Penetration of *Salmonella* through a polarized Madin-Darby canine kidney epithelial cell monolayer. J. Cell Sci. **107:**221–230.
9. **Francis, C. L., M. N. Starnbach, and S. Falkow.** 1992. Morphological and cytoskeletal changes in epithelial cells occur immediately upon interaction with *Salmonella typhimurium* grown under low-oxygen conditions. Mol. Microbiol. **6:**3077–3087.
10. **Galán, J. E.** 1994. *Salmonella* entry into mammalian cells: different yet converging signal transduction pathways? Trends Cell Biol. **4:**196–199.
11. **Galán, J. E., J. Pace, and M. J. Hayman.** 1992. Involvement of the epidermal growth factor receptor in the invasion of cultured mammalian cells by *Salmonella typhimurium*. Nature (London) **357:**588–589.
12. **Ginocchio, C., J. Pace, and J. E. Galán.** 1992. Identification and molecular characterization of a *Salmonella typhimurium* gene involved in triggering the internalization of salmonellae into cultured epithelial cells. Proc. Natl. Acad. Sci. USA **89:**5976–5980.
13. **Jones, B. D., H. F. Paterson, A. Hall, and S. Falkow.** 1993. *Salmonella typhimurium* induces membrane ruffling by a growth factor-receptor-independent mechanism. Proc. Natl. Acad. Sci. USA **90:**10390–10394.
14. **McEwan, G. T. A., M. A. Jepson, B. H. Hirst, and N. L. Simmons.** 1993. Polycation-induced enhancement of epithelial paracellular permeability is independent of tight junction characteristics. Biochim. Biophys. Acta **1148:** 51–60.
15. **Pace, J., M. J. Hayman, and J. E. Galán.** 1993. Signal transduction and invasion of epithelial cells by *S. typhimurium*. Cell **72:**505–514.
16. **Peterson, M. W., and D. Gruenhaupt.** 1990. A23187 increases permeability of MDCK monolayers independent of phospholipase activation. Am. J. Physiol. **259:**C69–C76.
17. **Ruschkowski, S., I. Rosenshine, and B. B. Finlay.** 1992. *Salmonella typhimurium* induces an inositol phosphate flux in infected epithelial cells. FEMS Microbiol. Lett. **95:**121–126.
18. **Shasby, D. M., M. Winter, and S. S. Shasby.** 1988. Oxidants and conductance of cultured epithelial cell monolayers: inositol phospholipid hydrolysis. Am. J. Physiol. **255:**C781–C788.
19. **Takeuchi, A.** 1967. Electron microscope studies of experimental salmonella infection. Am. J. Pathol. **50:**109–136.